Characterization of rockfall mechanisms and run-out in active volcano-tectonic areas: a case study from Ischia Island, Southern Italy

Massaro, L.[1,2], Rauseo, F.[1], De Falco, M.[1], Marino, E.[1], Forte, G.[1], Santo, A.[1]

[1]Department of Civil, Architectural and Environmental Engineering, Università degli Studi di Napoli Federico II, Naples, Italy

[2]Department of Earth Sciences, Royal Holloway University of London, Egham, United Kingdom

Introduction and geological setting

Ischia is a volcanic island of the Phlegrean Volcanic District (Southern Italy) that was recently affected by multiple geological hazards, including floodings, landslides, rockfall and earthquakes.

In this study, rockfall stability is analysed for the site of Frassitelli, Forio d'Ischia, which is an area of high residential, touristic and agricultural importance. The study area is a 400 m-wide cliff made of Green Tuff (Fig. 1), located on the western area of Mt. Epomeo and composed of two step-like outcrops located at 420 (cliff A) and 280 (cliff B) m a.s.l., respectively.

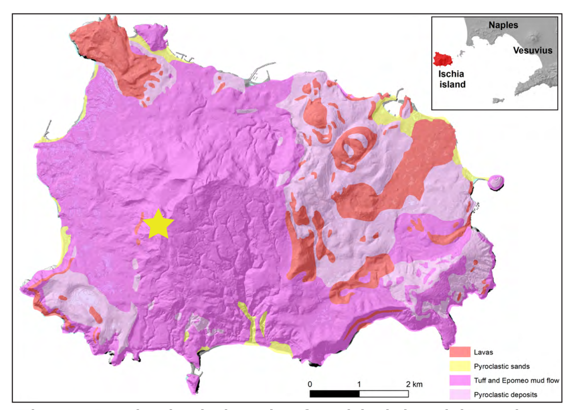

Fig. 1. Geological sketch of Ischia island (Southern Italy) and location of the study area (yellow star in the map).

The field survey allowed the collection of geostructural data and the UAV image acquisition. The latter enabled the construction of Virtual Outcrop Models (VOM), aimed at characterising the fracture systems affecting the examined area. Subsequently, the structural analysis of the area provided insights into the most critical sectors for the numerical models of rockfall propagation. The modelling was performed with the software RAMMS::ROCKFALL, developed by Leine et al. (2014). Different rock volume and shape scenarios were investigated and the results were discussed in terms of hazard with respect to the local residential area.

Structural analysis

The drone-acquired images enabled the development of the orthomosaic map (fig. 2a) and the VOMs of the two analysed outcrops (fig. 2b). The former allowed the identification of the rock blocks at the base of the slopes and the estimation of the volumes.

The structural data of the faults and fractures characterising the study area were collected from field surveys and VOMs. The latter were analysed with the software OpenPlot (Tavani et al., 2011), which enabled the digitisation of the structural features (fig. 2b). The dataset from field and VOM surveys permitted to define the rock mass discontinuity sets, which are characterised by the presence of three principal sets of fractures (stereographic plot in fig. 2b): J1, N-S (272/72); J2, NW-SE (218/75); J3, NE-SW (325/80).

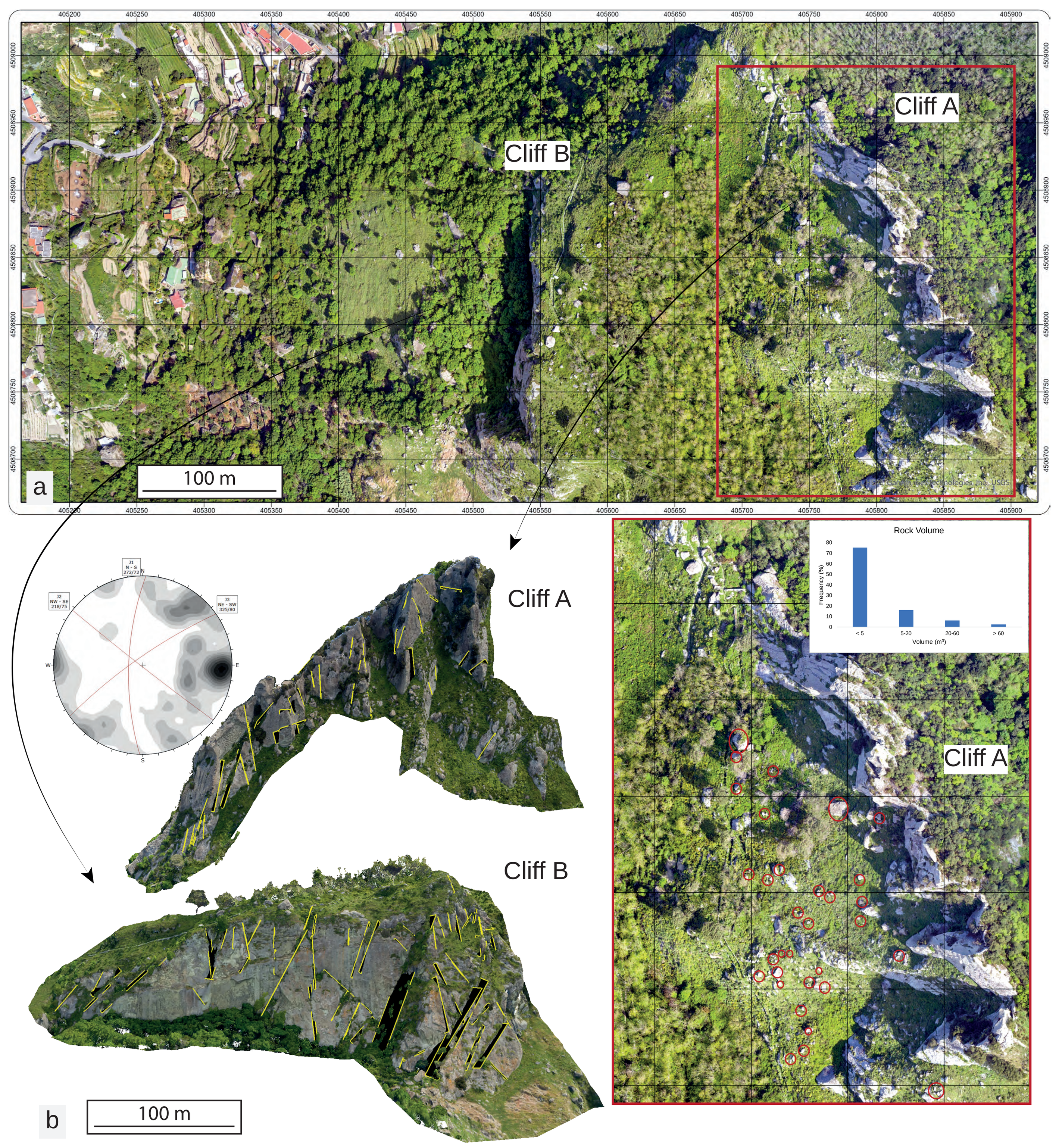

Fig. 2. Examined area and outcrops. a) Orthomosaic map developed from drone-acquired images and used to collect the volumes of the rock blocks at the base of the slope (rock volume frequency chart); b) VOMs of the two outcrops with the digitised fractures and stereographic representation of the collected data.

Structural analysis

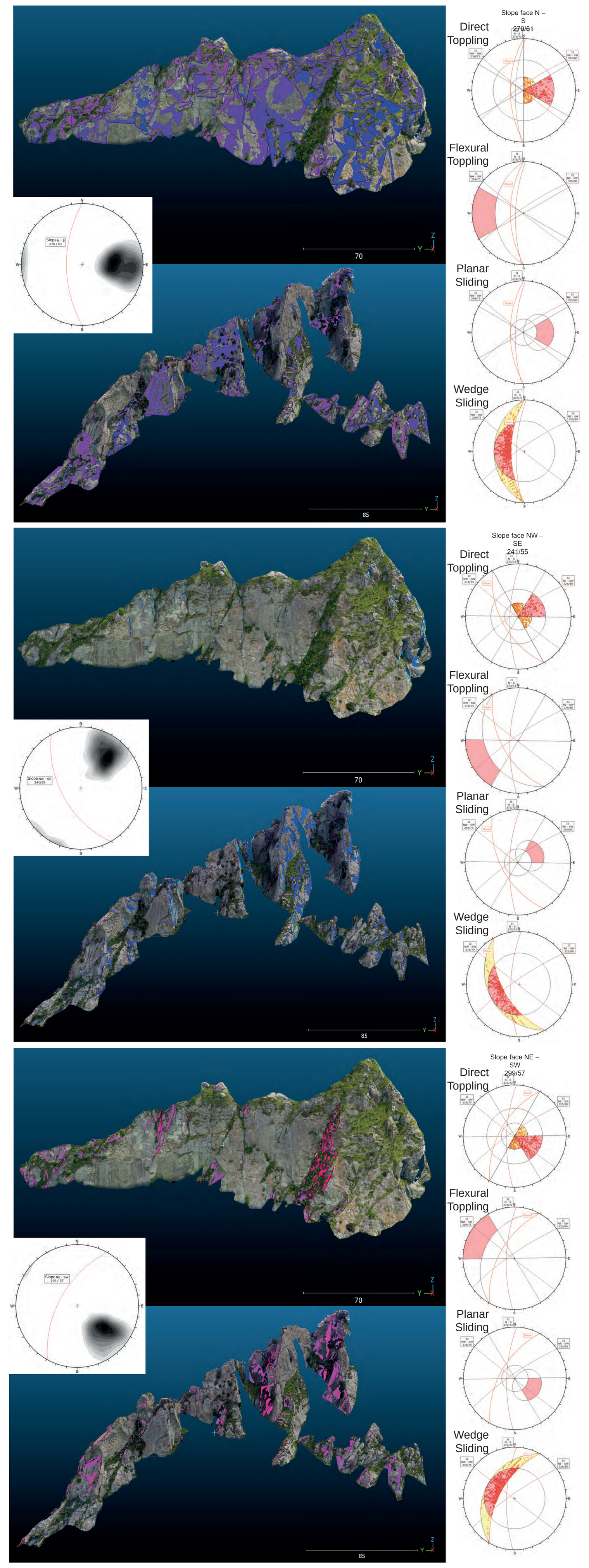

Fig. 3. Kinematic analysis performed for the three main slope faces defined with the 'Facets' plugin in CloudCompare software, with the respective stereographic projection. The kinematic analyses were performed for the potential failure mechanisms of direct toppling, flexural toppling, planar sliding and wedge sliding.

The VOMs were analysed with the software CloudCompare by applying the plugin 'Facets' (Dewez et al., 2016). The latter enabled the automatic measurement of the slope faces, allowing the reconstruction of the outcrop geometries. Three main slope faces, validated by field survey data, were defined, striking N-S, NW-SE, and NE-SW (fig. 3).

Successively, the kinematic analyses of the potential failure mechanisms were performed for each of the three slope faces, based on the collected fracture dataset (fig. 3).

The results of the kinematic analysis are summarised in fig. 4. The wedge sliding is the most likely failure mechanism on all the slope faces, with percentages of critical intersections of 23%, 21%, and 11% on the N-S, NE-SW, and NW-SE slope faces, respectively. Comparable values of critical intersections are observed only for the planar sliding (9% on the N-S slope face and 7% on the NE-SW slope face) and for the flexural toppling (9% on the NW-SE slope face).

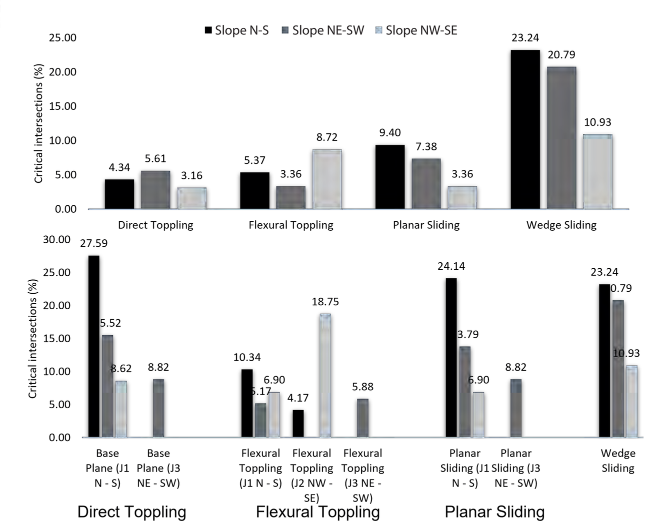

Fig. 4. Kinematic analysis results quantified as the percentage of critical intersections a) within the fracture network and b) per fracture set.

Rockfall simulations: methods

The rockfall trajectory simulations with RAMMS::ROCKFALL software were performed in different scenarios of volume and shape of the rock blocks, with the following workflow:

- the geomorphological characteristics of the slope were derived from the UAV-based DEM (1 m x 1 m resolution);
- from the structural analysis, the critical areas of failure were defined as well as the range of rock volumes potentially involved in a rockfall event. Three volume classes were used: 5, 20, and 60 m³;
- the lithological units were defined, assigning a 'Terrain Category' with specific friction parameters (Table 1);
- three shapes of the rock blocks were used (fig. 5), based on the observations derived from the structural analysis and aimed at evaluating the influence of the shape on the rockfall trajectories.

Terrain Category	μ_{min}	μ_{max}	β	k	$C_v (m^{-1})$
Soft	0.25	2	100	1.25	0.8
Medium	0.35	2	150	2	0.6
Medium Hard	0.4	2	175	2.5	0.5

Forest Category	Basal Area
Medium Forest	$35 \frac{m^3}{ha}$

Table 1. Friction parameters for the terrain categories used in the simulations.

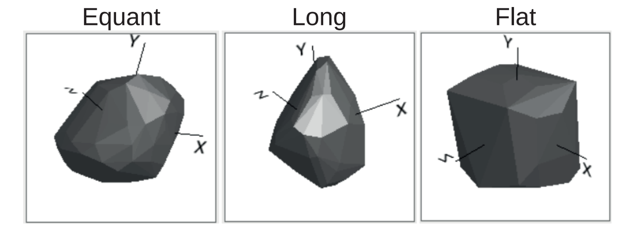

Fig. 5. Shapes of the rock blocks used in the rockfall simulations.

Rockfall simulations: results

The combination of the defined rock volumes and shapes provided 9 different scenarios, which were simulated with fixed input parameters to ensure equal comparison (Table 2).

A total of 50 release points were defined for each of the two outcrops. The number of random orientations was arbitrarily set to 20 (total launched rock blocks per model = 2000).

Input parameters	
Initial velocity (m s⁻¹)	0.02
Initial rotational velocity (rad s⁻¹)	0.00
n. of random orientations	20
n. of release points	50

Scenario	Volume (m³)	Shape	Density (kg m³)
1	5	Equant	2200
2	5	Long	2200
3	5	Flat	2200
4	20	Equant	2200
5	20	Long	2200
6	20	Flat	2200
7	60	Equant	2200
8	60	Long	2200
9	60	Flat	2200

Table 2. Input parameters and specifics of the rockfall simulations.

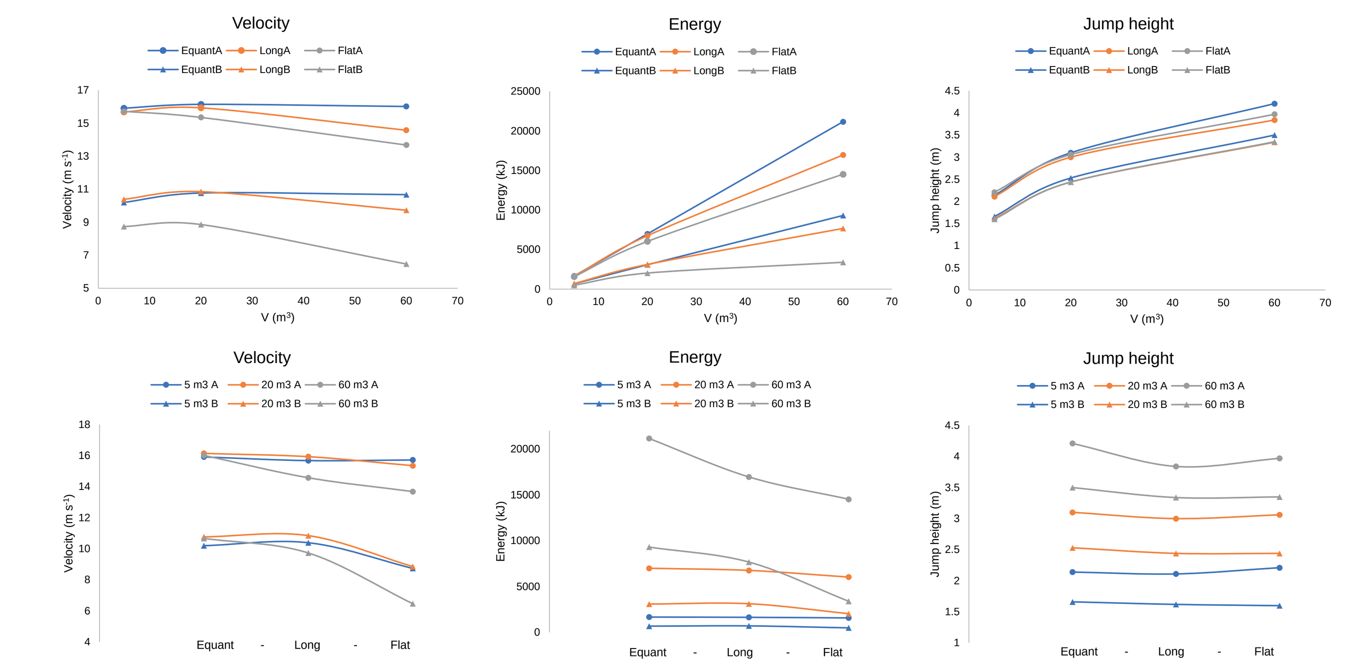

Fig. 6. Quantitative output data representing the median of the simulated trajectories from the 9 modelled scenarios. a) velocity (m s⁻¹), kinetic energy (kJ), and jump height (m) of the rock blocks as a function of the rock block volume (m³). b) velocity (m s⁻¹), kinetic energy (kJ), and jump height (m) of the rock blocks as a function of the rock block shape.

The different scenarios simulated and the comparison of the results enabled defining the influence of the volume and shape of the rock blocks on the characteristics of the trajectories (fig.6).

The velocity is poorly influenced by the volume of the rock blocks, especially for cliff A. The shape of the blocks shows an impact on the velocity of the rock blocks with high volumes (60 m³).

A positive linear relationship between kinetic energy and rock volume is observed. On the other hand, the shape influences the kinetic energy of the rock blocks only with high volumes. In the 60 m³ case, the equant blocks have the highest energy and the flat blocks display the lowest median value of energy.

The jump height increases with higher volumes but is poorly influenced by the shape of the blocks. Overall, the rock blocks of the higher outcrop (cliff A) show higher values of velocity, kinetic energy and jump height with respect to those falling from cliff B.

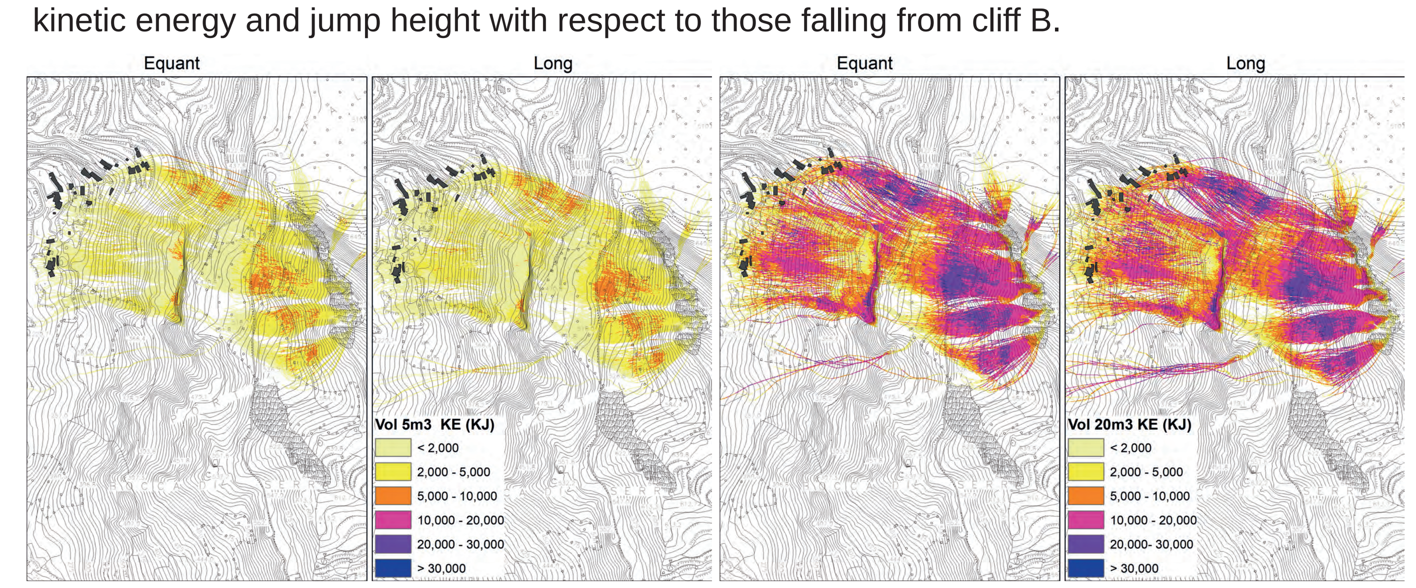

Fig. 7. Trajectory maps displaying the values of kinetic energy (kJ) of the rock blocks for the 'equant 5 m³', 'long 5 m³', equant 20 m³', and 'long 20 m³' scenarios. The buildings of the residential area are indicated in black.

The 60 m³ scenarios were simulated to evaluate the impact of the rock volume on the rockfall trajectories, considering such a rock volume as potentially mobilised only in the case of seismically induced rockfall events. Similarly, the 'flat' shape was considered less likely to occur and was simulated mainly to investigate the impact of the block shape on the rockfall trajectories. Therefore, in the final maps the following scenarios are represented:

- Equant 5 m³;
- Long 5 m³;
- Equant 20 m³;
- Long 20 m³.

The kinetic energy trajectory maps (fig. 7) show the impact, in terms of energy (kJ), that the potential rock blocks could have in the residential area. The cliff of the lower outcrop (cliff B) represents a natural barrier for most of the rock blocks falling from cliff A. However, in the northern sector of cliff B, this natural barrier is not sufficiently consistent and the rock blocks find a preferential path, as displayed by the trajectories. Moreover, in this northern sector, the buildings of the residential area are proximal to the examined outcrops.

Discussions

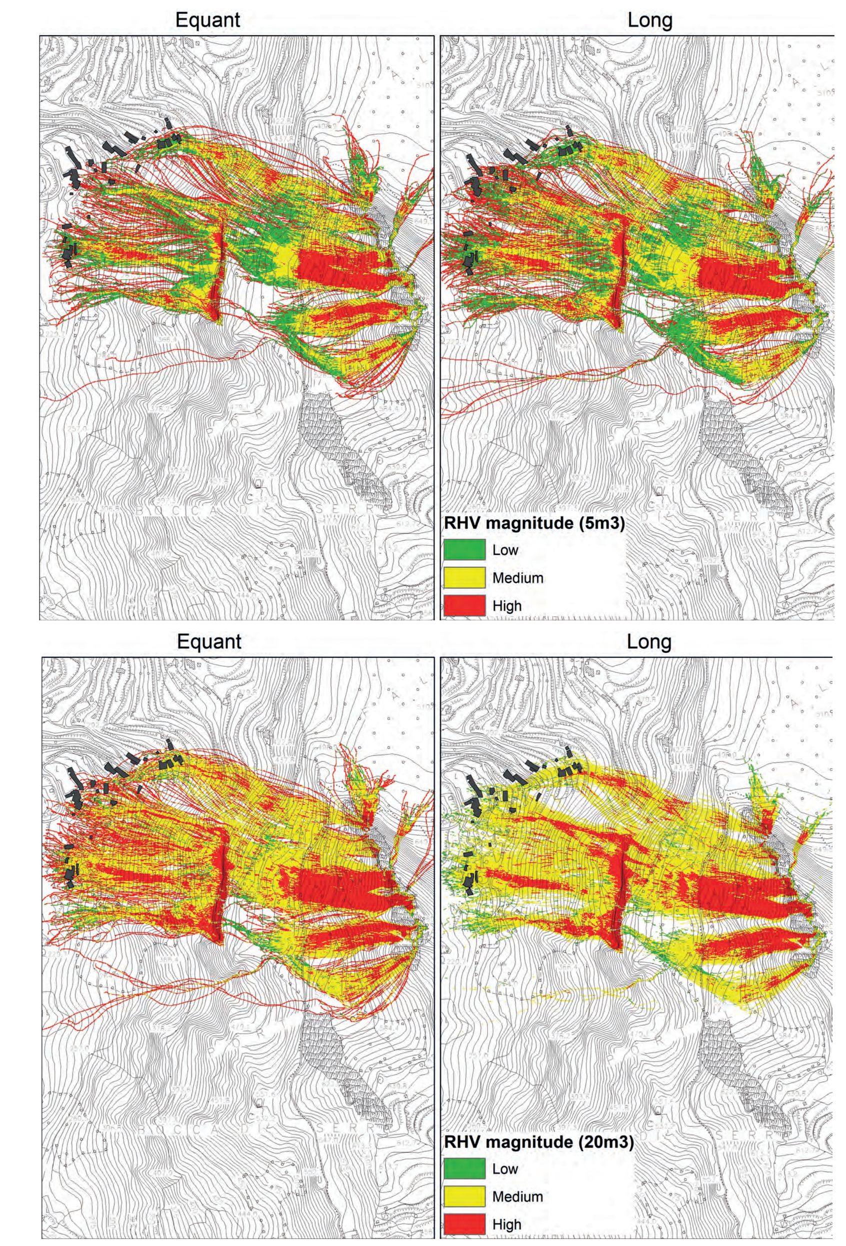

The parameters obtained from the rockfall simulations allowed the calculation of the Rockfall Hazard Vector (RHV) magnitude as defined in Crosta & Agliardi (2003) (fig. 8). This parameter calculation is based on the kinetic energy, jump height, and number of blocks.

The percentage of rock blocks (fig. 9a) and the percentage of 'RHV magnitude' (fig. 9b) with respect to the urban area are summarised for the four final models. The 'long 20 m³' model shows the highest percentage of blocks reaching the buildings (37%), while the 'equant 20 m³' the lowest (16%). However, the 'long 20 m³' model displays only 0.8% of high RHV in the urban area. The latter value is higher for the 'long 5 m³' and the 'equant 20 m³' models (10%).

Fig. 8. Trajectory maps displaying the RHV magnitude of the rock blocks for the 'equant 5 m³', 'long 5 m³', equant 20 m³', and 'long 20 m³' scenarios. The buildings of the residential area are indicated in black.

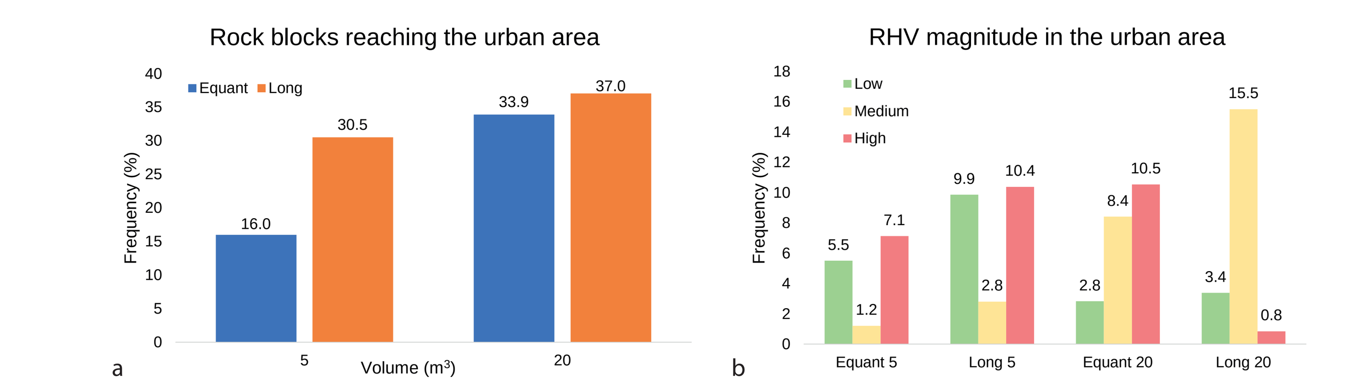

Fig. 9. a) percentage of rock blocks reaching the residential area (with respect to the total number of blocks launched) and b) percentage of RHV magnitude with resepct to the total residential area.

Conclusions

From the structural analysis and the rockfall simulations performed on two outcrops of Mt. Epomeo (Ischia island) the following observations were made:

- the examined area is characterised by three main sets of fractures, striking N-S, NW-SE, and NE-SW;
- the most likely failure mechanism is the wedge sliding;
- the rockfall simulations showed that the volume of the rock blocks has a direct influence on the kinetic energy and jump height of the rock trajectories;
- the shape of the rock blocks has an impact on the velocity and kinetic energy only with high rock volumes (60 m³) and has no evident influence on the jump height;
- the rock blocks reach the residential area with a maximum kinetic energy of about 2000 kJ and 10000 kJ in the 5 m³ and 20 m³ models, respectively;
- in the 'long 5 m³', 'equant 20 m³' and 'long 20 m³' scenarios, 30%, 34% and 37%, respectively, of the rock blocks reach the urban area;
- in the 'long 5 m³' and 'equant 20 m³' models, 10% of the urban area has a high RHV magnitude;
- in general, the northern sector of the residential area is more affected by cliff A, whereas the rock blocks reaching the southern urban area belong to cliff B;
- the risk of rockfalls affecting the residential area could be mitigated by applying artificial barriers with rock volume scenarios up to 20 m³, while with higher volumes involved, a timely evacuation would represent the suitable action.

References

Crosta, G.B., Agliardi, F., 2003. A methodology for physically based rockfall hazard assessment. Nat. Hazards Earth Syst. Sci. 3, 407-422.

Dewez, T.J.B., Girardeau-Montaut, D., Allanic, C., Rohmer, J., 2016. FACETS : A CLOUDCOMPARE PLUGIN TO EXTRACT GEOLOGICAL PLANES FROM UNSTRUCTURED 3D POINT CLOUDS. Int. Arch. Photogramm. Remote Sens. Spatial Inf. Sci. XLI-B5, 799-804.

Leine, R.I., Schweizer, A., Christen, M., Glover, J., Bartelt, P., Gerber, W., 2014. Simulation of rockfall trajectories with consideration of rock shape. Multibody System Dynamics 32, 241-271.

Tavani, S., Arbues, P., Snidero, M., Carrera, N., Muñoz, J.A., 2011. Open Plot Project: an open-source toolkit for 3-D structural data analysis. Solid Earth 2, 53-63.